

# Deeply inelastic scattering off nuclei at RHIC

Raju Venugopalan

*Physics Department and RIKEN-BNL Research Center, BNL, Upton, NY 11973, USA*

## Abstract

We discuss the physics case for an electron–nucleus collider at RHIC.

# 1 Introduction

A high energy electron–nucleus collider, with a center of mass energy  $\sqrt{s} = 60$ – $100$  GeV, presents a remarkable opportunity to explore fundamental and universal aspects of QCD. The nucleus, at these energies, acts as an amplifier of the novel physics of high parton densities— aspects of the theory that would otherwise only be explored in an electron–proton collider with energies at least an order of magnitude greater than that of HERA. An electron–nucleus collider will also make the study of QCD in a nuclear environment, to an extent far beyond that achieved previously, a quantitative science. In particular, it will help complement, clarify, and reinforce physics learnt at high energy nucleus–nucleus and proton–nucleus collisions at RHIC and LHC over the next decade. For both of these reasons, an eA collider facility represents an important future direction in high energy nuclear physics.

We will summarize here the physics arguments that support both the key points above. We will also briefly discuss experimental observables in deeply inelastic scattering (DIS) and signatures of novel physics. Accelerator and detector issues have been discussed elsewhere. Details on these, on the physics issues, and references to an extensive literature can be found in proceedings [1, 2] of two of the three eRHIC workshops that were held in the last year <sup>1</sup> and in the earlier proceedings of eA HERA workshops [3].

The physics arguments can be separated according to the kinematic regions of interest <sup>2</sup>. Very roughly, these are

- the small  $x_{Bj}$  region ( $x_{Bj} < 1/(2m_N R_A) \approx 0.01$  for a large nucleus), where the virtual photon interacts coherently with partons in a nucleus over a region exceeding its longitudinal extent  $2R_A$ .

---

<sup>1</sup>More information on eRHIC and on previous eA studies for HERA can also be found at the website: <http://quark.phy.bnl.gov/raju/eRHIC.html>

<sup>2</sup> $m_N$  below is the nucleon mass.

- the intermediate  $x_{Bj}$  region ( $1/(2m_N R_A) < x_{Bj} < 1/(2m_N R_N) \approx 0.1$  for a large nucleus), where the virtual photon interacts coherently over longitudinal distances larger than the longitudinal size of the nucleon  $2R_N$ , but smaller than the longitudinal size of the nucleus  $2R_A$ .
- the large  $x_{Bj}$  region ( $x_{Bj} > 1/(2m_N R_N) \approx 0.1$  for a large nucleus) where the virtual photon/W or Z boson is localized within a longitudinal distance smaller than the nucleon size.

In this talk, we will cover only the physics of the small  $x_{Bj}$  region. Due to space limitations, we will not cover the interesting physics at intermediate  $x_{Bj}$  that can be studied with an eA collider. This covers the region in  $x_{Bj}$  from where inter-nucleon forces become important to coherent effects involving several nucleons. A nice discussion of these issues (in the context of the HERA eA collider proposal) can be found in Ref. [3]. We will not discuss the physics of the large  $x_{Bj}$  region either—this topic has been covered by other participants at this meeting [4].

## 2 eA physics at small $x_{Bj}$ : $x_{Bj} < 1/(2m_N R_A)$

This regime of small  $x_{Bj}$ 's ( $x_{Bj} \leq 0.01$ ) is easily accessed by an electron–heavy ion collider in the energy range  $\sqrt{s} \approx 60$ –100 GeV. Fig. 1 is a plot of the  $x - Q^2$  plane delineating the range mapped for  $\sqrt{s} = 63$  GeV (10 GeV electrons on 100 GeV heavy ions at RHIC). What is novel about these energies is that for the first time one can study the physics of  $x_{Bj} \ll 0.01$  in a nucleus for  $Q^2 \gg \Lambda_{QCD}^2$ , where  $\Lambda_{QCD} \sim 200$  MeV. Previous (fixed target) experiments such as NMC and E665 and current ones such as HERMES and COMPASS could only access small  $x_{Bj}$  at small  $Q^2$ 's.

Some questions that may come immediately to mind are:

- i) why is it important to simultaneously have large  $Q^2$  at small  $x_{Bj}$  ?

ii) Hasn't HERA explored this  $x_{Bj}-Q^2$  range already? What then can one learn by studying the same regime with an eA collider?

iii) In the nuclear context, haven't the fixed target experiments at CERN, DESY and Fermilab, studied the small  $x_{Bj}$  regime?

iv) Does the collider environment have a compelling advantage in the study of small  $x_{Bj}$  physics?

In the following, we will address in detail the physics issues that underly these queries. The pithy answer to all of these however is that *an eA collider in the desired energy range may probe a hitherto inaccessible regime of QCD, where the properties of strongly interacting matter are radically different from those studied previously*. Understanding the properties of QCD in this regime may provide us the answer to fundamental questions about the strong interactions that remain unanswered. A brief list of these open questions is: a) what is the nature of multi-particle production? b) how do cross-sections behave at high energies? Are the bulk features of the cross-section computable in QCD? c) Are the properties of hadrons universal at very high energies? d) what is the nature of confinement-in particular, as probed in striking phenomena such as hard diffraction? and e) what are the initial conditions for heavy ion collisions, and how do they affect the formation of a quark gluon plasma?

We will also emphasize that mapping the relevant  $x - Q^2$  regime with the proposed collider, at the high luminosities considered, will provide measurements of several physical quantities, with a much higher degree of precision, and of course in a wider kinematic range. Aside from their intrinsic interest, these quantities will be extremely important for the physics goals of other current and future experiments.

## 2.1 Why is it important to simultaneously have large $Q^2$ and small $x_{Bj}$ ?

In deeply inelastic scattering (DIS), one has the exact kinematic relation

$$y x_{Bj} = Q^2/s.$$

All of these variables are invariants—they are frame independent. The invariants  $x_{Bj}$  and  $Q^2$  are of course well known – they are simply related, respectively, to the fraction of the momentum of a hadron or nucleus carried by a parton, and to the momentum transfer squared from the electron to the hadron. The invariant  $y$ , in the rest frame of the target, is the ratio of the energy transferred to the hadron to the energy of the electron. It has the kinematic range  $0 \leq y \leq 1$ . For the purposes of this discussion, we will assume that  $y \sim 1$ , or  $x_{Bj} \sim Q^2/s$ <sup>3</sup>.

The physics of small  $x$  is the physics of high energies<sup>4</sup>. The total cross-section in strong interaction physics can be parametrized by the power law behavior  $\sigma(s) \sim s^\epsilon$ , where  $\epsilon \sim 0.08$ . Thus the cross-section grows with decreasing  $x$  and, at high energies, is dominated by small  $x$ . This behaviour is explained in Regge phenomenology via Pomeron exchange—the  $t$ -channel exchange of an object with vacuum quantum numbers. Though the Pomeron hypothesis has had some striking success [7] in explaining high energy data, and has been the paradigm for understanding non-perturbative multi-particle production, it is not clear that it can be interpreted as an actual particle and understood as arising from the fundamental theory. A popular construction, first postulated by Francis Low and Shmuel Nussinov [6], is that the Pomeron is two gluon exchange with vacuum quantum numbers in the  $t$  channel.

---

<sup>3</sup>How large a value of  $y$  can be obtained without being swamped by uncertainties in the radiative corrections is a very important technical issue we will not address here. It has been addressed previously in proceedings of the eA at HERA workshops. These can be accessed on the World Wide Web at the URL: <http://www.desy.de/~heraws96/proceedings/>

<sup>4</sup>For a review of recent theoretical developments, see Ref. [5].

However, since total cross-sections at lower energies than available currently were dominated by very soft transverse momenta, it proved very hard to come up with a robust QCD based theory of the Pomeron (or more generally, that of the behavior of the bulk of the cross-section at high energies), that would also have predictive power.

The situation has changed with the advent of colliders at very high energies. With the Hadron Electron Ring Accelerator (HERA) at DESY, where 27.5 GeV electrons collide with 920 GeV protons, corresponding to a center of mass energy  $\sqrt{s} \sim 300$  GeV, one can have  $Q^2 = 1\text{--}10$  GeV<sup>2</sup> for  $x_{Bj} \sim 10^{-4}$ . In prior experiments, at these low  $x_{Bj} \sim 10^{-4}$ , only  $Q^2 \ll \Lambda_{QCD}^2$  could be accessed. Thus even though one was probing the small  $x_{Bj}$  regime of the Pomeron, the coupling constant was too large to make predictions and therefore test/extract information about the theory in this regime. Since QCD is enormously complex, the lack of a small parameter in this regime was problematic. It hobbled progress in small  $x_{Bj}$  physics even though a wealth of tantalizing small  $x_{Bj}$  data [3] exists at small  $Q^2$ . A large number of models were constructed to understand the data, but their connection to the fundamental theory is still tenuous.

At HERA, the coupling  $\alpha_S(Q^2) \ll 1$  in a significant portion of the small  $x_{Bj}$  regime of interest. Since the coupling is weak, computations can be made in pQCD and tested against the data. It lead, for instance, to the resurrection of the idea of the perturbative Pomeron developed by Lipatov and colleagues in the late 1970's—now known by the acronym BFKL Pomeron [9]. In QCD, a Pomeron can be constructed from the exchange of gluon ladders—the so-called hard Pomeron. The leading order BFKL result predicts rising cross-sections that rise more rapidly than the HERA data support. The next to leading order correction is very large and negative, thereby causing great confusion (and interest) in the QCD community [10, 11]. One possibility is a more subtle resummation of next-to-leading order small  $x$  effects in the BFKL framework [12]; another is to formulate the problem of QCD at small

$x_{Bj}$  in the language of high parton densities—thereby performing a different sort of resummation [13, 14, 15]. This topic will be addressed in the following sub-section.

The ability to probe large  $Q^2$ 's at small  $x_{Bj}$  has thus given us a handle on understanding, in a quantitative way, the hitherto inaccessible small  $x_{Bj}$  regime of QCD. This represents tremendous progress since it is this regime of the theory that controls the bulk of high energy cross-sections. Without understanding this regime, one cannot claim reliably that one completely understands the theory.

In what follows, we will discuss what we have learnt from the HERA experiments in the small  $x_{Bj}$  and large  $Q^2$  regime, and how these experiments point to novel physics that may be fully explored with an eA collider.

## 2.2 From HERA towards a new regime of high parton densities

The wide kinematic range in  $x$  and  $Q^2$  of the HERA collider can be seen in Fig. 1. One of the striking results from HERA is that the gluon distribution, extracted from scaling violations of  $F_2$ , grows rapidly at small  $x$  and high  $Q^2 \gg \Lambda_{QCD}^2$ . This is shown in Fig. 2. This tells us that at high energies the proton is not a simple object with three valence quarks and a few gluons that bind together the quarks. At a fixed external scale  $Q^2 = 20 \text{ GeV}^2$ , one finds 25–30 gluons, per unit rapidity, at  $x_{Bj} = 10^{-4}$  in the proton. The proton is therefore very rapidly growing dense as the resolution scale in  $x$  is shifted to smaller  $x$ 's.

At high  $Q^2$ , ( $Q^2 \gg 10 \text{ GeV}^2$ ) the rise in the gluon structure function at small  $x$  is very well understood [16] in the framework of perturbative QCD (pQCD). An asymptotic expression for the rise is the double logarithmic formula where the gluon distribution grows as

$$G(x, Q^2) \sim \exp \left[ \sqrt{\ln \left( \ln \left( \frac{Q^2}{\Lambda_{QCD}^2} \right) \right) \ln(1/x)} \right], \quad (1)$$

This double logarithmic behavior was tested at HERA. It is claimed that the value of  $\alpha_S(Q^2)$  extracted from the fit provides a precise determination of the coupling

at  $M_Z \sim 91$  GeV and is in agreement with other world data [17]. More detailed NLO QCD fits with different sets of parton distributions [18] have been shown to describe the HERA data for a wide range of  $x_{Bj}$  and  $Q^2$ . At high  $Q^2$ , the deeply inelastic scattering data is a testament to the striking success of perturbative QCD.

In the very high  $Q^2$  regime— $Q^2 \gg 10$  GeV<sup>2</sup>, one is not probing the region of extremely small  $x_{Bj}$ : for  $Q^2 = 10$  GeV<sup>2</sup>, the smallest  $x_{Bj}$  available is  $\sim 10^{-4}$ . In the region of  $Q^2 = 1\text{--}10$  GeV<sup>2</sup>, at correspondingly smaller  $x_{Bj}$ , the situation from the usual pQCD standpoint is less clear [19, 20]. The HERA ZEUS and H1 QCD fits agree with the data but with the price being that one extracts an anomalously small value of the gluon distribution, and one obtains more sea quarks than glue at small  $x$  [21, 22]. The anomalously small gluon distribution is seen in Fig. 2 for  $Q^2 = 1$  GeV<sup>2</sup> where, at small  $x$ , the distribution is consistent with zero. Several groups have argued that one obtains results that run contrary to our intuition because the standard pQCD approach is breaking down <sup>5</sup>. The Tel Aviv group of Gotsman et al., for instance, claims that there is no pQCD fit that can simultaneously explain the inclusive  $F_2$  data and the large amount of data on the energy dependence of  $J/\psi$  photo-production [24]. For a recent discussion of unitarity and long distance effects in  $J/\psi$  photo-production, see Ref. [25].

The argument is that screening effects due to large parton densities are important in this regime and have to be taken into account. The physics is still weak coupling though; one still has  $\alpha_S \ll 1$  in the  $Q^2 = 1\text{--}10$  GeV<sup>2</sup> regime. Phenomenological models that take these effects into account, and match into the usual pQCD formalism at high  $Q^2$ , have been successful in fitting both the inclusive and the diffractive HERA data [26, 27, 28, 29].

There are therefore tantalizing hints from the HERA data that one is beginning to see the effects of large parton densities in the proton. We will argue below that

---

<sup>5</sup>For a summary of recent discussions, see Ref. [23].



standard pQCD breaks down when the parton densities become very large. Even though the coupling is weak, the physics will be non-perturbative due to the high field strengths generated by the large number of partons. This is a novel regime of the theory. We will further argue that an eA collider is much better suited to explore this regime even though its  $x$ - $Q^2$  range will be somewhat less extensive than that achieved at HERA.

### 2.3 QCD is a colored glass condensate at high energies

In the infinite momentum frame (IMF), the number of partons per unit transverse area, for a fixed resolution of the external probe  $Q^2 \gg \Lambda_{QCD}^2$ , grows rapidly with the energy—or with decreasing  $x_{Bj}$ . In this high parton density regime, the corresponding QCD field strength squared <sup>6</sup> becomes  $F_{\mu\nu}^2 \sim 1/\alpha_S$ : since  $\alpha_S(Q^2) \ll 1$ , the color field strengths in this regime are large [30]. The non-linearities inherent in the theory become manifest, radically altering the properties of distributions in high energy collisions. For instance, the gluon distribution that was growing slowly now saturates—and grows very slowly—at most logarithmically with decreasing  $x_{Bj}$ .

In this high parton density—large field strengths—regime, the saturated gluons, when viewed in the IMF, form a novel state of matter which we will henceforth call a color glass condensate (CGC) [31]. Why a glass, and why a condensate? At small  $x_{Bj}$ , most of the partons are rapidly fluctuating gluons that interact weakly with each other. They are however strongly coupled to the large  $x_{Bj}$  “hard” parton color charges, that act as random, static, sources of color charge. This is exactly analogous to a glassy system—in particular, one can show that there is a formal analogy to spin glass condensed matter systems [32]. In the latter case, one has a disordered state of spins coupled, say, to random magnetic impurities—in the “quenched” limit, these impurities are static—or long lived.

---

<sup>6</sup> $F_{\mu\nu}^2$  is frame independent.

Further, since the occupation number of the gluons is large, they form a condensate. Being bosons, arbitrary numbers of gluons can pile up in a momentum state. In the classical Bose gas, for instance, Bose–Einstein condensation leads to a dramatic overpopulation of the zero momentum state. In our case, since the gluons are interacting, and have both attractive and repulsive interactions, they “pile” up in a narrow band of states, peaked at a typical momentum we shall call the “saturation” momentum [15, 33, 34, 35]. The saturation scale at a particular  $x$  is the density per unit area of all the parton sources at higher  $x$ ’s. One has

$$Q_s^2(x) = \frac{1}{\pi R^2} \frac{dN}{d\eta}, \quad (2)$$

Here  $\eta = \ln(1/x)$  is the rapidity. As the energy increases, or  $x_{Bj}$  decreases, this “bulk” scale of the condensate grows and one can have  $Q_s \gg \Lambda_{QCD}$ . The distinction between fields and sources is of course arbitrary—as one decreases  $x$ , what were formerly fields turn into sources—thereby increasing the density of sources. This transformation is nothing but the “block spin” renormalization group transformation of Wilson, and the equations describing the evolution to small  $x_{Bj}$  are Wilsonian renormalization group equations [33, 36]. There has been significant theoretical progress recently in understanding the asymptotic behavior of these renormalization group equations [37].

Thus, because a large scale  $Q_s$  is generated at small  $x$ , one can predict the behavior of this non–perturbative condensate using weak coupling QCD techniques. An interesting question we don’t have the answer to yet is how the coupling constant behaves in this regime—is there a fixed point of the theory at high energies? It would be therefore be absolutely remarkable, and of fundamental interest, if it could be demonstrated empirically that QCD at very high energies is a non–trivial glassy condensate of gluons.

In Fig. 3, is plotted a (very) schematic diagram of scattering in the  $\eta = \ln(1/x)$  versus  $Q^2$  plane. If  $x_{Bj}$  is not too small, and  $Q^2$  is large, the Dokshitzer–Gribov–

Lipatov–Altarelli–Parisi (DGLAP) QCD evolution equations [38] work very well. For a fixed  $Q^2$ , the Balitsky–Fadin–Kuraev–Lipatov (BFKL) equations describe the  $x$  evolution of distributions in a limited kinematic range. Both of these are linear evolution equations and do not fully take into account the non-linearities of the theory. Indeed, with regard to the latter, it is not clear there is a physical kinematical region available for linear evolution, where these equations apply, before high parton density effects set in. The line in the  $\eta$ - $Q^2$  plane represents the scale  $Q_s(x)$  that separates the extensively studied regime of the well known QCD evolution equations from the saturation regime of the CGC.

We discussed in the previous sub-section how the HERA data may be showing hints of screening effects that may be the precursor to the saturation regime. We will argue below that deep inelastic scattering off large nuclei at high energies may be sufficient to probe this novel regime of the theory.

## 2.4 Probing the colored glass condensate in eA DIS

At a high energy eA collider, with energies  $\sqrt{s} = 60$ – $100$  GeV, one will access (roughly)  $x_{Bj} = 10^{-4}$ – $10^{-3}$  for, respectively,  $Q^2 = 1$ – $10$  GeV<sup>2</sup>—see Fig. 1. These values of  $x_{Bj}$  and  $Q^2$  are in the ballpark (even if more limited in range) than those at HERA. However, an eA collider has a tremendous advantage—the parton density in a nucleus, as experienced by a probe at a fixed energy, is much higher than what it would experience in a proton at the same energy. Since the parton density grows as  $A^{1/3}$ , this effect is more pronounced for the largest nuclei. To probe a comparable parton density in a nucleon, the probe would have to be at much higher energies than presently available.

The physics behind this effect is subtle and is a result of quantum coherence. In DIS at small  $x_{Bj}$ , in the target rest frame, the virtual photon splits into a quark–anti-quark pair, that subsequently interacts with the nucleus. If  $x_{Bj} \ll 1/(2m_N R_A) \sim 0.01$ , the  $q\bar{q}$  pair interacts coherently with partons along the entire

length of the nucleus. Furthermore, equally importantly, if the transverse separation of the pair  $\sim 1/Q$  is smaller than the nucleon size ( $Q^2 > \Lambda_{QCD}^2$ ), the probe will experience, coherently, random  $p_t$  kicks from partons in different nucleons along its trajectory. While  $\langle p_t \rangle \sim 0$ , fluctuations will be large:  $\langle p_t^2 \rangle \sim A^{1/3}$ . In the IMF, this effect is interpreted as the  $q\bar{q}$ -pair experiencing large fluctuations of color charge in the nuclear “pancake”. It is clear, from both viewpoints, that a large scale, proportional to the parton density per unit area, is generated in large nuclei due to quantum mechanical coherence at small  $x_{Bj}$  and large  $Q^2$ . This scale is none other than the saturation scale  $Q_s(x)$  discussed previously.

In a nucleus, one defines

$$Q_s^2 = \frac{1}{\pi R^2} \frac{dN}{dy} \equiv \frac{A^{1/3}}{x^\delta} \text{fm}^{-2}, \quad (3)$$

Here  $\delta$  is the power of the rise in the gluon distribution in a *nucleon* at the typical  $Q^2 \sim Q_s^2$  of interest <sup>7</sup>. At HERA, for  $Q^2$  of a few  $\text{GeV}^2$ , a reasonable estimate is  $\delta \sim 0.3$ . Now if we ask at what  $x_{Bj}$  in a proton will the probe see the same parton density as in a nucleus, Eq. 3 suggests,

$$x_{\text{proton}} = \frac{x_{\text{nucleus}}}{\left(A^{1/3}\right)^{1/\delta}}. \quad (4)$$

Since the nucleus is dilute, and if, being conservative, we assume that one can’t tag on impact parameter—we take the effective  $A^{1/3} = 4$ , then for  $\delta \sim 0.3$ , we find  $x_{\text{proton}} \sim x_{\text{nucleus}}/100$ . Thus, one would obtain the same parton density in a nucleus at  $x_{Bj} \sim 10^{-4}$  and  $Q^2 \sim$  a few  $\text{GeV}^2$ , as would be attained in a *nucleon* at  $x_{Bj} \sim 10^{-6}$  and similar  $Q^2$ ! Put differently, it would take an electron–proton collider with an order of magnitude larger energy than HERA to achieve the same parton density as would be achieved by eRHIC. It is now believed that impact parameter tagging is feasible by counting knock-out neutrons [39, 40]—if so, the gain in parton density in eA relative to ep would be even more spectacular.

---

<sup>7</sup> This scale must be determined self-consistently.

The small  $x_{Bj}$  regime has been studied previously in fixed target DIS off nuclei at CERN and Fermilab. In these experiments, the center of mass energy was a factor of 3–5 less than the proposed collider. This corresponds to a factor of 10–25 smaller in  $Q^2$  for the same  $x_{Bj}$ . It was therefore difficult to interpret the experimental results at small  $x_{Bj}$  in the framework of perturbative QCD. Remarkable phenomena, such as shadowing, were observed—the relation of the experimentally measured shadowing to the physics of parton saturation presented here is at present unclear and deserves to be explored further. It could not be explored at the fixed target experiments because the kinematics corresponded to an intrinsically non-perturbative regime of the theory that is not amenable to a weak coupling perturbative QCD based analysis upon which the parton saturation picture rests.

In the following, we will discuss both inclusive and semi-inclusive signatures of the CGC. The latter, in particular, are striking. In this regard as well, the collider environment holds a significant edge since semi-inclusive observables proved very difficult to measure in fixed target eA DIS.

## 2.5 Signatures of the new physics of the CGC

A number of inclusive and semi-inclusive experimental observables exist that will be sensitive to the new physics in the regime of high parton densities. All the inclusive and semi-inclusive observables that were studied at HERA can be studied with eRHIC—with a ZEUS/H1 type detector design [40]. However, due to the remarkable versatility of RHIC, and due to likely improvements in detector design, several new observables can be measured in the small  $x_{Bj}$  region for the first time. We will first discuss inclusive variables and the signatures of new physics in these. We will then discuss semi-inclusive observables.

### Inclusive signatures of the CGC

An obvious inclusive observable is the structure function  $F_2(x_{Bj}, Q^2)$  and its

logarithmic derivatives with respect to  $x_{Bj}$  and  $Q^2$ . eRHIC should have sufficient statistical precision for one to extract the logarithmic derivatives of  $F_2$  (and of its logarithmic derivatives!). Whether the systematic errors at small  $x_{Bj}$  will affect the results is not clear at the moment.

The logarithmic derivative  $dF_2/d\ln(Q^2)$ , at fixed  $x_{Bj}$ , and large  $Q^2$ , as a function of  $Q^2$ , is the gluon distribution. QCD fits implementing the DGLAP evolution equations should describe its behavior at large  $Q^2$ . At smaller  $Q^2$ , one should see a significant deviation from linear QCD fits—in principle, if the  $Q^2$  range is wide enough, one should see a turnover in the distribution. The  $Q^2$  at which the turnover takes place should be systematically larger for smaller  $x$ 's and for larger nuclei. Predictions for this quantity, as a function of  $Q^2$ , for fixed  $W^2$  and for fixed  $x$ , in a phenomenological model, are shown in Figs. 4 and 5 respectively.

A remarkable feature of eRHIC will be that one can extract the longitudinal structure function  $F_L(x_{Bj}, Q^2) = F_2 - 2x_{Bj}F_1$  at small  $x_{Bj}$  for the first time. An independent extraction of  $F_L$  requires that the energy of the colliding beams be varied significantly. At RHIC, this is feasible. In the parton model,  $F_L = 0$ —thus  $F_L$  is very sensitive to scaling violations. In particular, it provides an independent measure of the gluon distribution—a fact that makes this quantity very important to measure in its own right [41].

It has been suggested by several authors that  $F_2 = F_L + F_T$  is not very sensitive to higher twist saturation effects which may be prominent in both  $F_L$  and  $F_T$  but may cancel in the sum [42]. An independent measurement of  $F_L$ , and thereby of  $F_T$ , will confirm this claim. The ratio of  $F_L/F_T$  has a very particular behavior in screening/saturation models. In Figs. 6 and 7 is shown the prediction from a particular model for this ratio [43]. The ratio  $F_L/F_T$ , for a fixed  $x_{Bj}$ , has a maximum at a particular  $Q^2$ ; this maximum grows with the nuclear size (Fig. 6). As  $x_{Bj}$  decreases, the position of the maximum, for each nucleus, increases (Fig. 7). The maximum at which the turnover  $Q_{eff}(x, A)$  occurs is related to the saturation

scale  $Q_s$ . The precise relation is not known currently independently of particular models. To study the  $A$  dependence, it might be more useful to look at  $F_L$  and  $F_T$  separately.

A very important inclusive observable is nuclear shadowing. Quark shadowing is defined through the measured ratio of the nuclear structure function  $F_2^A$  to  $A$  times the nucleon structure function  $F_2^N$ :  $S_{\text{quark}} = F_2^A / AF_2^N$ . Gluon shadowing is similarly defined to be  $S_{\text{gluon}} = G_A / AG_N$ . Quark shadowing was observed in the fixed target experiments (NMC, E665, ...) and gluon shadowing, indirectly, through logarithmic derivatives of  $F_2$ . However, the gluon shadowing data at the smallest  $x$ 's are also at very low  $Q^2$ —where the application of perturbative QCD is unreliable.

There are model calculations (see Fig. 8) that suggest that gluon shadowing is very large at small  $x_{Bj}$ 's and fairly large  $Q^2$  [28]. eRHIC can help confirm if this is the case. In addition, because of the extended kinematic range of eRHIC, we can determine whether shadowing is entirely a leading twist phenomenon, or if there are large higher twist perturbative corrections. Some saturation models, for instance, predict that perturbative shadowing will become large as one goes to smaller  $x_{Bj}$ 's [46]. Isolating perturbative contributions to shadowing from non-perturbative ones will be an interesting experimental and theoretical challenge. Another interesting question is whether shadowing saturates at a particular value of  $x_{Bj}$ , for fixed  $Q^2$  and  $A$ . How does this value vary with  $x_{Bj}$  and  $Q^2$ ? Does the ratio of quark shadowing to gluon shadowing saturate?

Finally, it is well known that there is a close relation between shadowing and diffraction. See Fig. 9. Whether this relation persists at high parton densities is not known. In an interesting recent exercise, it has been shown that diffractive *nucleon* data at HERA could be used to predict the shadowing of quark distributions observed by NMC [47, 56]. Significant deviations from the simple relation between shadowing and diffraction, may again suggest the presence of strong non-linearities. At eRHIC the validity of this relation can be explored directly—different nuclear

targets are available, and the diffractive structure function may also be measured independently.

### Semi-inclusive signatures of the CGC

The discussion of the relation between shadowing and diffraction provides a smooth segue into the topic of semi-inclusive signatures of the Colored Glass Condensate. While the novel physics of saturation and the formation of a CGC should be visible in inclusive quantities, their most dramatic manifestation will be in semi-inclusive measurements.

The most striking of these semi-inclusive measurements is hard diffraction. Hard diffraction is the phenomenon wherein the virtual photon emitted by the electron fragments into a final state  $X$ , with an invariant mass  $M_X^2 \gg \Lambda_{QCD}^2$ , while the proton emerges unscathed in the interaction. A large rapidity gap—a region in rapidity essentially devoid of particles—is produced between the fragmentation region of the electron and that of the proton. In pQCD, the probability of a gap is exponentially suppressed as a function of the gap size. At HERA though, gaps of several units in rapidity are unsuppressed; one finds that roughly 10% of the cross-section corresponds to hard diffractive events with invariant masses  $M_X > 3$  GeV. The remarkable nature of this result is transparent in the proton rest frame; a 50 TeV electron slams into the proton and, 10% of the time, the proton is unaffected, even though the interaction causes the virtual photon to fragment into a hard final state.

The interesting question in diffraction is to study the nature of the color singlet object (the “Pomeron”) within the proton that interacts with the virtual photon since it addresses, in a novel fashion, the central mystery of QCD—the nature of confining interactions within hadrons. In hard diffraction, the mass of the final state is large and one can reasonably ask questions about the quark and gluon content of the Pomeron. A diffractive structure function  $F_{2,A}^{D(4)}$  can be defined [48, 49, 50], in



a fashion analogous to  $F_2$ , as

$$\frac{d^4\sigma_{eA\rightarrow eXA}}{dx_{Bj}dQ^2dx_{\mathcal{P}}dt} = A \cdot \frac{4\pi\alpha_{em}^2}{xQ^4} \left\{ 1 - y + \frac{y^2}{2[1 + R_A^{D(4)}(\beta, Q^2, x_{\mathcal{P}}, t)]} \right\} F_{2,A}^{D(4)}(\beta, Q^2, x_{\mathcal{P}}, t), \quad (5)$$

where,  $y = Q^2/sx_{Bj}$ , and analogously to  $F_2$ , one has  $R_A^{D(4)} = F_L^{D(4)}/F_T^{D(4)}$ . Also,

$$Q^2 = -q^2 > 0; \quad x_{Bj} = \frac{Q^2}{2P \cdot q}; \quad x_{\mathcal{P}} = \frac{q \cdot (P - P')}{q \cdot P}; \quad t = (P - P')^2, \quad (6)$$

and  $\beta = x_{Bj}/x_{\mathcal{P}}$ . Here  $P$  is the initial nuclear momentum, and  $P'$  is the net momentum of the fragments  $Y$  in the proton fragmentation region. Similarly,  $M_X$  is the net momentum of the fragments  $X$  in the electron fragmentation region. An illustration of the hard diffractive event is shown in Fig. 10. Unlike  $F_2$  however,  $F_2^{D(4)}$  is not truly universal—it cannot be applied, for instance, to predict diffractive cross-sections in  $p$ - $A$  scattering; it can be applied only in other lepton-nucleus scattering studies [50].

It is more convenient in practice to measure the structure function  $F_{2,A}^{D(3)} = \int F_{2,A}^{D(4)} dt$ , where  $|t_{min}| < |t| < |t_{max}|$ , where  $|t_{min}|$  is the minimal momentum transfer to the nucleus, and  $|t_{max}|$  is the maximal momentum transfer to the nucleus that still ensures that the particles in the nuclear fragmentation region  $Y$  are undetected. An interesting quantity to measure is the ratio

$$R_{A1,A2}(\beta, Q^2, x_{\mathcal{P}}) = \frac{F_{2,A1}^{D(3)}(\beta, Q^2, x_{\mathcal{P}})}{F_{2,A2}^{D(3)}(\beta, Q^2, x_{\mathcal{P}})}. \quad (7)$$

For eA at HERA, it was argued that this ratio could be measured with high systematic and statistical accuracy [3]—the situation for eRHIC should be at least comparable, if not better. If  $R_{A1,A2} = 1$ , one can conclude that the structure of the Pomeron is universal, and one has an  $A$ -independent Pomeron flux. If  $R_{A1,A2} = f(A1, A2)$ , then albeit a universal Pomeron structure, the flux is  $A$ -dependent. Finally, if Pomeron structure is  $A$ -dependent, some models argue that  $R_{A1,A2} = F_{2,A1}/F_{2,A2}$ .

We discussed previously that the ratio of  $R_D = \sigma_{\text{diffractive}}/\sigma_{\text{total}}$  at HERA is  $\sim 10\%$  for  $M_X > 3$  GeV. The systematics of hard diffraction at HERA can be understood in saturation models [26]. For eA collisions at eRHIC energies, saturation models predict that the ratio  $R_D^A$  can be much higher—on the order of 30% for the largest nuclei [51, 52]. The appearance of a large rapidity gap in 30% of all eA scattering events would be a striking confirmation of the saturation picture. Much theoretical and experimental work needs to be done to flesh out the details of predictions for hard diffractive events at eRHIC. Recent estimates suggest, for instance, that  $F_L^D/F_T^D$ , like  $F_L/F_T$  may have a peak as a function of  $Q^2$ , whose position, likewise, increases with decreasing  $x_{Bj}$  and increasing  $A$  [43].

An important semi-inclusive observable in eA DIS at high energies is coherent (or diffractive) and inclusive vector meson production. As discussed by Brodsky et al. [44] (see also Ref. [45]), the forward vector meson diffractive lepton production cross-section off nuclei

$$\frac{d\sigma}{dt}\Big|_{t=0}(\gamma^*A \rightarrow VA) \propto \alpha_S^2(Q^2) \left[ G_A(x, Q^2) \right]^2, \quad (8)$$

for large  $Q^2$ . Here  $V$  denotes the vector meson. This quantity is clearly very sensitive to the gluon structure function. The ratio of this quantity in nuclei to that in nucleons is therefore (like the ratio of the longitudinal structure function) a probe of gluon shadowing.

In the color dipole picture, the amplitude for diffractive lepton production can be written as a convolution of the  $q\bar{q}$  component of the  $\gamma^*$  wavefunction times the  $q\bar{q}$ -nucleus cross-section times the vector meson wavefunction. In the saturation picture, a semi-hard scale is introduced via the  $q\bar{q}$ -A cross-section—whether this scale is larger or smaller than the scale associated with the size of the vector meson strongly affects the energy and  $Q^2$  dependence of the vector meson cross-sections at small  $x_{Bj}$ . Recently, Caldwell and Soares [53] have studied vector meson production at HERA in the Golec-Biernat-Wusthoff model of saturation [26]. They find that

the model provides a good description of the cross-section for photo-and electro-production of  $J/\Psi$  in a wide  $Q^2$  and energy range. For  $\rho$  meson production, the change in the energy dependence as a function of  $Q^2$  is well described by the model but the normalization of the cross-section is not. One possible explanation of this discrepancy is the lack of knowledge about the  $\rho$  wavefunction.

We should mention here that it is very important to measure inclusive and diffractive open charm and jets since they provide useful and independent measures of the gluon distribution (and gluon shadowing) at small  $x_{Bj}$ . These will complement information on the gluon structure functions obtained from the  $\ln(Q^2)$  derivative of  $F_2$ , from  $F_L$ , and from diffractive leptonproduction of vector mesons.

We may conclude from the above that it is in the measurement of semi-inclusive observables that a future collider environment has a marked superiority over previous fixed target electron-nucleus experiments. Rapidity gaps in eA collisions will be measured for the first time. Coherent and incoherent vector meson production can be studied in great detail in a wide kinematic range with much greater accuracy than previously.

At small  $x_{Bj}$ , the high parton densities produce large color fluctuations which are subsequently reflected in large multiplicity fluctuations. One expects for instance the following phenomena: a) a broader rapidity distribution in larger nuclei relative to lighter nuclei and protons, b) Rapidity correlations over several units of rapidity—an anomalous multiplicity in one rapidity interval in an event would be accompanied by an anomalous multiplicity in rapidity intervals several units away [54, 55] and c) a correlation between the central multiplicity with the multiplicity of neutrons in a forward neutron detector [56].

## 2.6 Precision measurements of nuclear observables at small $x_{Bj}$

In much of our discussion, we have focused on the potential of an eA collider to discover a novel state of saturated gluonic matter—the colored glass condensate.

This search, if successful, could revolutionize our understanding of QCD at high energies by providing answers to questions about the nature of confinement in high energy scattering, the origins of multi-particle production, the asymptotic behavior of cross-sections, etc.

However, even in the absence of the promise of radically new physics, there is a compelling case to be made for an eA collider. The gluon distribution in a nucleus is ill-understood. Understanding its behavior as a function of  $x_{Bj}$  and  $Q^2$ , and of its shadowing is of intrinsic interest. At eRHIC, as discussed above, measurements of  $F_L$ , and of semi-inclusive quantities promise that the gluon distribution in a nucleus could be independently extracted with high precision. The nuclear gluon distribution extracted with an eA collider can be compared with the distribution extracted from AA and pA collisions.

The  $A$  dependence (as a function of  $x_{Bj}$  and  $Q^2$ ) of vector meson production at small  $x_{Bj}$  ] is also of intrinsic interest, as well of use in interpretations of pA and AA collisions—a particular example being that of  $J/\psi$  suppression.

Hard diffraction off nuclei has not been previously measured. At eRHIC, nuclear diffractive structure functions can be measured for the first time. The relation of these to  $F_2$  will, as discussed previously, provide new insight into the relation between diffraction and shadowing.

At intermediate  $x$ 's, an eA collider provides a laboratory to study the propagation of fast partons through nuclear matter. Color transparency and color opacity, which we have not discussed here, can be studied more extensively than previously [57]. Jet quenching, often cited as a signature of the quark gluon plasma in nuclear collisions [58], can be investigated in the cold nuclear environment of an eA collider [59] and compared to results from AA collisions.

## 2.7 Connections to pA and AA physics

We will very briefly discuss here the relation of the physics of an eA collider to pA and AA physics at current and future collider facilities.

### Relation of eA to pA

In pA scattering at RHIC <sup>8</sup>, one also has the opportunity to study the gluon distribution in nuclei. Gluon fusion to jets, vector mesons, open charm and beauty can be measured. Hard and soft diffraction—the size and distribution of energy gaps with energy and nuclear size can also be studied. Scaling violations in Drell–Yan scattering can be measured for the first time.

Some of the differences between pA and eA are as follows. In pA scattering, for instance in the signature Drell–Yan process, it is very hard to reliably extract distributions in the region below the  $\Psi'$  tail—namely, one requires  $Q^2 > 16 \text{ GeV}^2$ . In the  $x$  region of interest, one expects saturation effects to be important at lower  $Q^2$  of 1–10  $\text{GeV}^2$ . For  $Q^2 = 16 \text{ GeV}^2$ , one might have to go to significantly smaller  $x$ 's to see large saturation effects. Secondly, the survival probability of large rapidity gaps is smaller in pA relative to eA. This is because the gap is destroyed due to secondary interactions between “spectator” partons in the proton and the “Pomeron” from the nucleus. This does not occur in eA scattering because of course there are no spectator partons in the electron. Thus one expects that diffractive vector meson and jet production in pA should be qualitatively different than what one will see in eA.

### Relation of eA to AA

A large variety of models combining hard and soft physics are used to study nuclear collisions at RHIC and LHC energies [60]. Many of these model predictions depend sensitively on the nuclear gluon density—for a recent parametrization of

---

<sup>8</sup>For a recent discussion, see the proceedings of the pA workshop at BNL, Oct. 28th–29th, Eds. S. Aronson and J. C. Peng, at the website [www.bnl.gov/rhic/townmeeting/agenda\\_b.htm](http://www.bnl.gov/rhic/townmeeting/agenda_b.htm)

nuclear gluon densities, see Ref. [61]. Data from an eA collider will be essential in further refining these parametrizations.

In the classical approach discussed previously, the relation between the parton distributions in the nuclear wavefunction and the multiplicity of produced gluons simplifies—the initial multiplicity of produced gluons is given in terms of the saturation scale  $Q_s$  by the simple relation [62]

$$\frac{1}{\pi R^2} \frac{dN}{d\eta} = c_N \frac{N_c^2 - 1}{N_c} \frac{1}{4\pi^2 \alpha_S} Q_s^2. \quad (9)$$

The coefficient  $c_N$  can be estimated numerically in classical lattice simulations of nuclear collisions [63] and is determined to be  $c_N \sim 1.3$ . A similar analysis is used to determine the initial energy of the produced glue [64]. This distribution is only the initial parton distribution—the subsequent possible evolution to a quark gluon plasma [65] is controlled again only by the scale  $Q_s$ .

It is therefore conceivable that high energy heavy ion collisions, despite their complexity, may provide insight into the parton distributions in the nuclear wavefunction. An eA collider will confirm and deepen our understanding of what we may learn from heavy ion collisions.

### 3 Summary

In this talk, we discussed the physics case for an eA collider. We emphasized the novel physics that might be studied at small  $x$ . The interesting physics at intermediate  $x$ 's has been discussed elsewhere [3].

Plans for an electron–ion collider include, as a major part of the program, the possibility of doing polarized electron–polarized proton/light ion scattering. A discussion of the combined case for high energy electron nucleus and polarized electron–polarized proton scattering will be published separately [66].

## 4 Acknowledgement

I would like to thank the organizers of the EPIC meeting at MIT for inviting me to present the physics case for eRHIC. Many thanks to Abhay Deshpande, Witek Krasny, Yuri Kovchegov, Genya Levin, Larry McLerran, and Mark Strikman for discussions, and for kindly allowing me to use figures from their papers. In particular, I would like to thank Mark Strikman for his detailed comments on the manuscript. I would also like to thank all the participants of the eA meeting at BNL in June/July 2000 for the stimulating discussions that have informed this report. This work was supported at BNL by the Department of Energy under DOE contract number DOE-FG02-93-ER-40764, by RIKEN-BNL, and by an LDRD grant from Brookhaven Science Associates.

## References

- [1] Proceedings of the 2nd eRHIC workshop, Yale, April 6th–8th, 2000, BNL–52592.
- [2] Proceedings of the BNL summer meeting, June 26th–July 14th, 2000, BNL–52606
- [3] M. Arneodo et al., in Proceedings of *Future Physics at HERA*, DESY, September 25th–26th, 1995, hep-ph/9610423.
- [4] proceedings of the EPIC meeting, MIT, Boston, September 14th–16th, 2000.
- [5] R. Venugopalan, *Pramana* **55**, 73 (2000) [hep-ph/0005096].
- [6] F. E. Low, *Phys. Rev. D* **12**, 163 (1975); S. Nussinov, *Phys. Rev. D* **14**, 246 (1976).

- [7] A. Donnachie and P. V. Landshoff, Phys. Lett. **B296**, 227 (1992) [hep-ph/9209205].
- [8] M. Arneodo, Phys. Rept. **240** (1994) 301.
- [9] E. A. Kuraev, L. N. Lipatov and V. S. Fadin, Sov. Phys. JETP**45**, 199 (1977);  
I. I. Balitsky and L. N. Lipatov, Sov. J. Nucl. Phys. **28**, 822 (1978).
- [10] V. S. Fadin and L. N. Lipatov, Phys. Lett. **B429**, 127 (1998) [hep-ph/9802290].
- [11] G. Camici and M. Ciafaloni, Phys. Lett. **B412**, 396 (1997) [hep-ph/9707390].
- [12] G. P. Salam, Acta Phys. Polon. **B30**, 3679 (1999) [hep-ph/9910492].
- [13] L. V. Gribov, E. M. Levin and M. G. Ryskin, Phys. Rept. **100**, 1 (1983).
- [14] A. H. Mueller and J. Qiu, Nucl. Phys. **B268**, 427 (1986).
- [15] L. McLerran and R. Venugopalan, Phys. Rev. D **49**, 2233 (1994); *ibid.*, 3352 (1994); Phys. Rev. D **50**, 2225 (1994); Phys. Rev. D **59**, 094002 (1999).
- [16] A. De Rujula, S. L. Glashow, H. D. Politzer, S. B. Treiman, F. Wilczek and A. Zee, Phys. Rev. D **10**, 1649 (1974); D. J. Gross, Phys. Rev. Lett. **32**, 1071 (1974).
- [17] R. D. Ball and S. Forte, Phys. Lett. **B358**, 365 (1995) [hep-ph/9506233].
- [18] H. L. Lai *et al.* [CTEQ Collaboration], Eur. Phys. J. **C12**, 375 (2000) [hep-ph/9903282]; A. D. Martin, R. G. Roberts, W. J. Stirling and R. S. Thorne, Nucl. Phys. Proc. Suppl. **79**, 105 (1999) [hep-ph/9906231]; M. Gluck, E. Reya and A. Vogt, Eur. Phys. J. **C5**, 461 (1998) [hep-ph/9806404].
- [19] L. Mankiewicz, A. Saalfeld and T. Weigl, hep-ph/9706330.
- [20] G. Altarelli, R. D. Ball and S. Forte, hep-ph/0011270.



- [21] J. Breitweg *et al.* [ZEUS Collaboration], Eur. Phys. J. **C6**, 43 (1999) [hep-ex/9807010].
- [22] C. Adloff *et al.* [H1 Collaboration], Z. Phys. **C76**, 613 (1997) [hep-ex/9708016].
- [23] M. F. McDermott, hep-ph/0008260.
- [24] E. Gotsman, E. Levin, M. Lublinsky, U. Maor, E. Naftali and K. Tuchin, hep-ph/0010198.
- [25] L. Frankfurt, M. McDermott and M. Strikman, hep-ph/0009086.
- [26] K. Golec-Biernat and M. Wusthoff, Phys. Rev. D **59**, 014017 (1999) [hep-ph/9807513]; *ibid.*, **60**, 114023 (1999) [hep-ph/9903358].
- [27] E. Gotsman, E. Levin, U. Maor and E. Naftali, Nucl. Phys. **B539**, 535 (1999) [hep-ph/9808257].
- [28] L. Frankfurt, V. Guzey and M. Strikman, J. Phys. **GG27**, R23 (2001) [hep-ph/0010248].
- [29] A. M. Stasto, K. Golec-Biernat and J. Kwiecinski, hep-ph/0007192.
- [30] A. H. Mueller, Lectures given at *International Summer School on Particle Production Spanning MeV and TeV Energies*, Nijmegen, Netherlands, 8-20 Aug 1999, hep-ph/9911289.
- [31] E. Iancu, A. Leonidov and L. McLerran, hep-ph/0011241.
- [32] G. Parisi and N. Surlas, Phys. Rev. Lett. **43**, 744 (1979).
- [33] J. Jalilian-Marian, A. Kovner, L. McLerran and H. Weigert, Phys. Rev. D **55**, 5414 (1997) [hep-ph/9606337].
- [34] Y. V. Kovchegov, Phys. Rev. D **54**, 5463 (1996) [hep-ph/9605446].

- [35] Y. V. Kovchegov and A. H. Mueller, Nucl. Phys. **B529**, 451 (1998) [hep-ph/9802440].
- [36] J. Jalilian–Marian, A. Kovner and H. Weigert, *Phys. Rev.* **D59** 014015 (1999).
- [37] I. Balitsky, *Phys. Rev.* **D60** 014020 (1999); *Phys. Rev. Lett.* **81** 2024 (1998); Y. V. Kovchegov, *Phys. Rev.* **D61**, 074018 (2000); E. Levin and K. Tuchin, hep-ph/9908317; E. Iancu, A. Leonidov and L. McLerran, hep-ph/0011241.
- [38] V. N. Gribov and L. N. Lipatov, Sov. J. Nucl. Phys. **15**, 78 (1972); G. Altarelli and G. Parisi, Nucl. Phys. **B126**, 298 (1977); Yu. L. Dokshitzer, Sov. Phys. JETP. **73**, 1216 (1977).
- [39] M. Strikman, M. G. Tverskoi and M. B. Zhalov, Phys. Lett. **B459**, 37 (1999) [nucl-th/9806099].
- [40] W. Krasny, contribution in Ref. 1.
- [41] A. Zee, F. Wilczek, and S. B. Treiman, Phys. Rev. D **10**, 2881 (1974); W. Bardeen, A. J. Buras, D. W. Duke, and T. Muta, Phys. Rev. D **18**, 3998 (1978).
- [42] J. Bartels, K. Golec-Biernat and K. Peters, Eur. Phys. J. **C17**, 121 (2000) [hep-ph/0003042].
- [43] E. Gotsman, E. Levin, U. Maor, L. McLerran and K. Tuchin, hep-ph/0008280; hep-ph/0007258.
- [44] S. J. Brodsky, L. Frankfurt, J. F. Gunion, A. H. Mueller and M. Strikman, Phys. Rev. **D 50**, 3134 (1994) [hep-ph/9402283].
- [45] B. Z. Kopeliovich, J. Nemchick, N. N. Nikolaev and B. G. Zakharov, Phys. Lett. **B324**, 469 (1994) [hep-ph/9311237].

- [46] J. Jalilian-Marian and X. Wang, Phys. Rev. D **60**, 054016 (1999) [hep-ph/9902411].
- [47] A. Capella, A. Kaidalov, C. Merino, D. Pertermann and J. Tran Thanh Van, Eur. Phys. J. **C5**, 111 (1998) [hep-ph/9707466].
- [48] A. Berera and D. E. Soper, Phys. Rev. D **53**, 6162 (1996) [hep-ph/9509239].
- [49] L. Trentadue and G. Veneziano, Phys. Lett. **B323**, 201 (1994).
- [50] J. C. Collins, Phys. Rev. D **57**, 3051 (1998) [hep-ph/9709499].
- [51] E. Levin and U. Maor, hep-ph/0009217.
- [52] L. Frankfurt and M. Strikman, *Phys. Lett.* **B382** (1996) 6.
- [53] A. C. Caldwell and M. S. Soares, hep-ph/0101085.
- [54] V. A. Abramovsky, V. N. Gribov and O. V. Kancheli, *Yad. Fiz.* **18**, 595 (1973).
- [55] Y. V. Kovchegov, E. Levin and L. McLerran, hep-ph/9912367.
- [56] L. Frankfurt and M. Strikman, Eur. Phys. J. **A5**, 293 (1999) [hep-ph/9812322].
- [57] L. Frankfurt, V. Guzey, W. Koepf, M. Sargsian and M. Strikman, hep-ph/9608492.
- [58] X. Wang, M. Gyulassy and M. Plumer, Phys. Rev. D **51**, 3436 (1995) [hep-ph/9408344].
- [59] R. Baier, Y. L. Dokshitzer, S. Peigne and D. Schiff, Phys. Lett. **B345**, 277 (1995) [hep-ph/9411409]; M. Luo, J. W. Qiu and G. Sterman, Phys. Rev. D **50**, 1951 (1994). E. Levin, Phys. Lett. **B380**, 399 (1996) [hep-ph/9508414].
- [60] N. Armesto and C. Pajares, *Int. J. Mod. Phys.* **A15**, 2019 (2000) [hep-ph/0002163].

- [61] K. J. Eskola, V. J. Kolhinen and C. A. Salgado, *Eur. Phys. J.* **C9**, 61 (1999) [hep-ph/9807297].
- [62] A. H. Mueller, *Nucl. Phys.* **B572**, 227 (2000) [hep-ph/9906322].
- [63] A. Krasnitz and R. Venugopalan, hep-ph/0007108, *Phys. Rev. Lett.* in press.
- [64] A. Krasnitz and R. Venugopalan, *Phys. Rev. Lett.* **84**, 4309 (2000) [hep-ph/9909203].
- [65] A. Dumitru and M. Gyulassy, *Phys. Lett.* **B494**, 215 (2000) [hep-ph/0006257]; J. Bjorker and R. Venugopalan, *Phys. Rev. C* **63**, 024609 (2001) [hep-ph/0008294]; R. Baier, A. H. Mueller, D. Schiff and D. T. Son, hep-ph/0009237.
- [66] A. Deshpande and R. Venugopalan, in preparation.

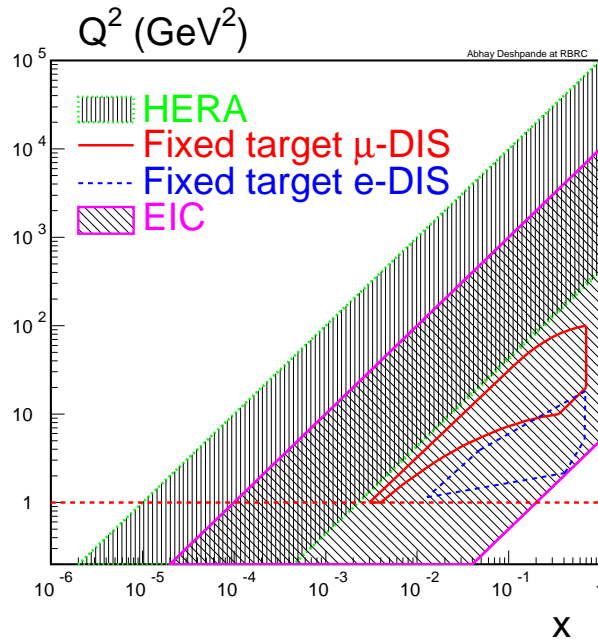


Figure 1: The  $x$ - $Q^2$  range of the electron ion collider (EIC) compared to that of the HERA ep collider and fixed target experiments. The EIC's reach would encompass the fixed target regime as well as part of the HERA regime.

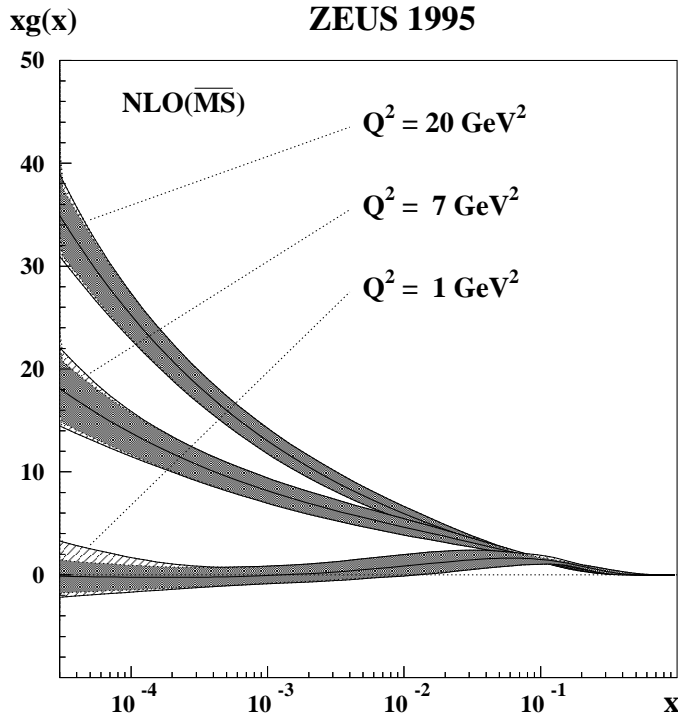


Figure 2: The gluon distribution for three different values of  $Q^2$  extracted using the ZEUS NLO QCD analysis. From Ref. [21].

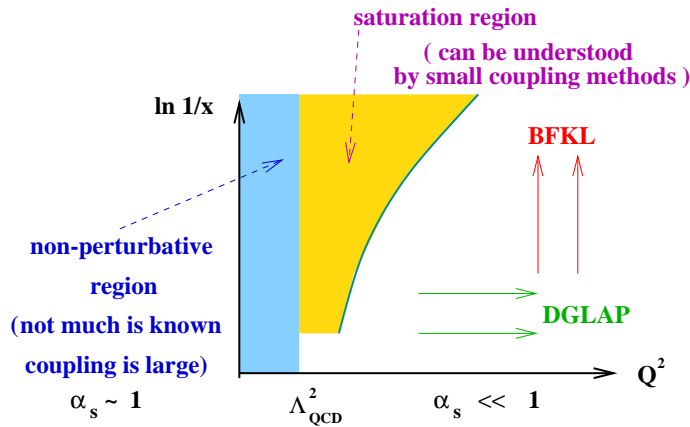


Figure 3: Schematic diagram of the  $\ln(1/x)-Q^2$  plane conveying a rough idea of the different regimes of applicability of the different evolution equations. Figure courtesy of Y. Kovchegov.

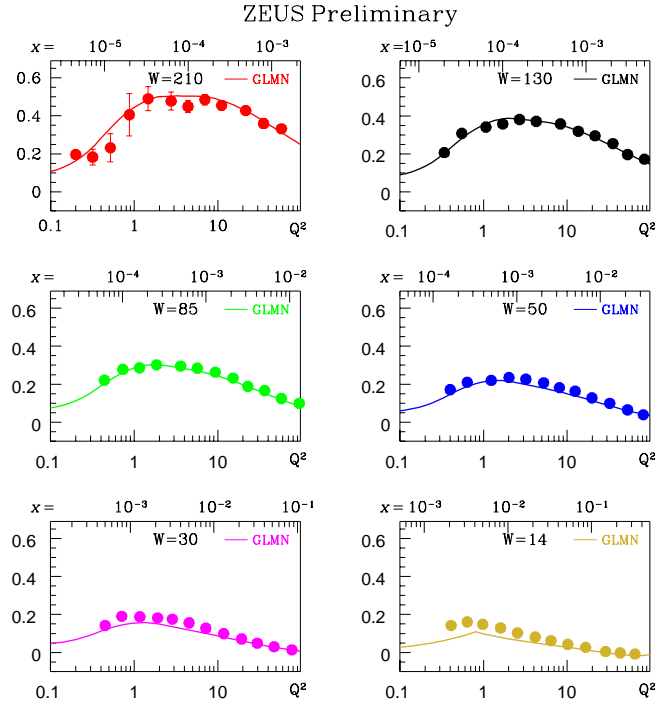


Figure 4: The slope  $dF_2/d\ln(Q^2)$  versus  $Q^2$  for fixed  $W^2$ . Figure from Ref. [24].

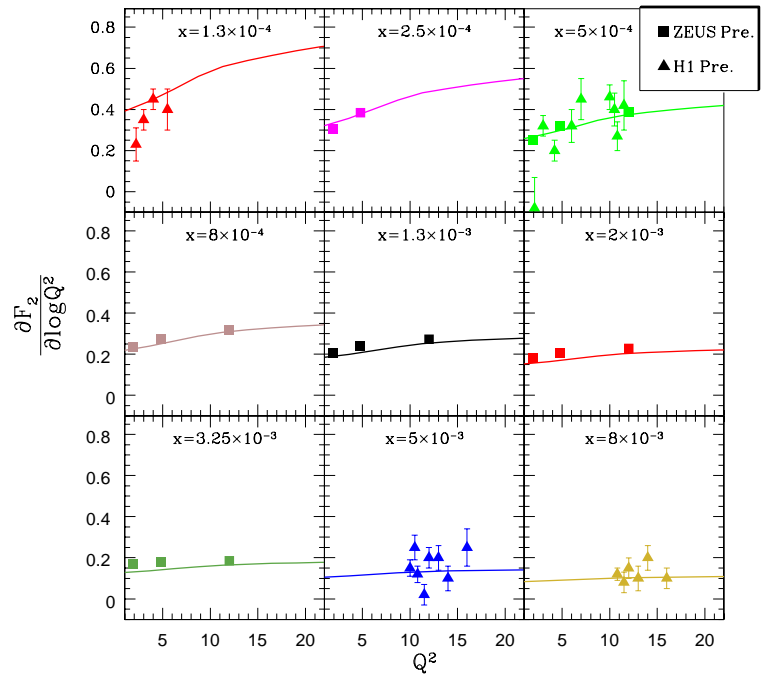


Figure 5: The slope  $dF_2/d\ln(Q^2)$  versus  $Q^2$  for fixed  $x$ .



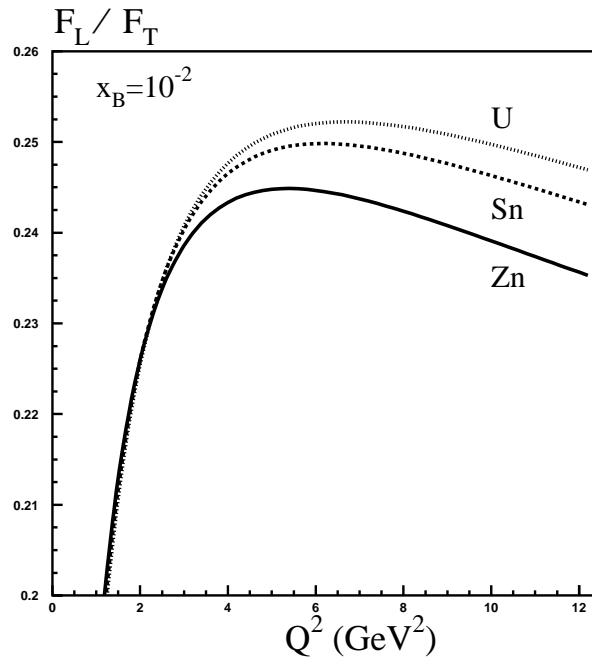


Figure 6: The ratio  $F_L/F_T$  as predicted in Ref. [43]. This ratio is plotted as a function of  $Q^2$  for different nuclei and for fixed  $x_{Bj}$ .

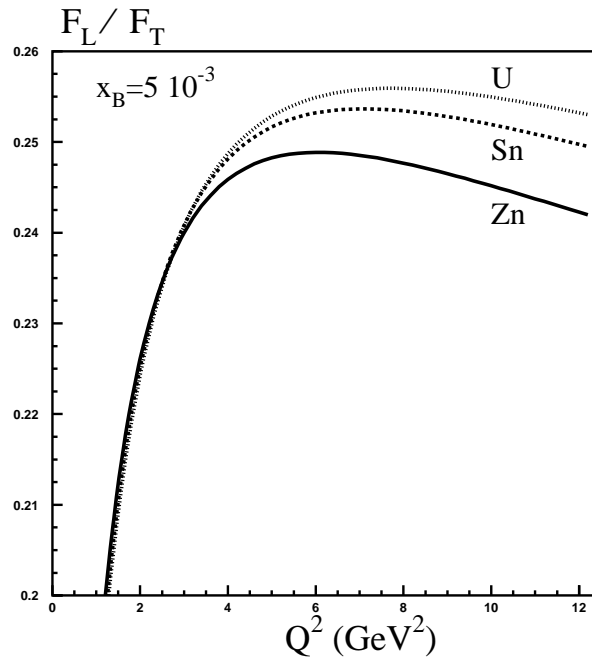


Figure 7: The ratio  $F_L/F_T$  as predicted in Ref. [43]. This ratio is plotted as a function of  $Q^2$  for different nuclei and for a different  $x_{Bj}$  than Fig. 6.

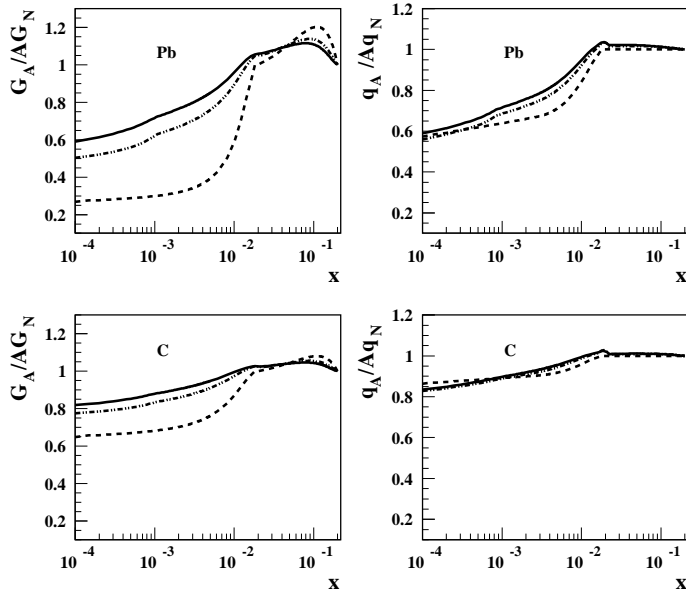


Figure 8: Gluon shadowing  $G_A(x, Q^2)/AG_N(x, Q^2)$  and quark shadowing  $q_A/Aq_N$  versus  $x_{Bj}$  for lead (Pb) and Carbon (C). The different curves correspond to  $Q = 2$  GeV (dotted),  $Q = 5$  GeV (dashed) and  $Q = 10$  GeV (solid). Figure from Ref. [28].

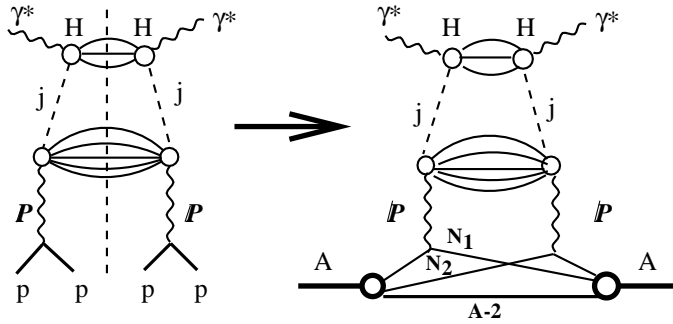


Figure 9: Diagrams demonstrating the relation between gluon induced hard diffraction on protons and the leading twist contribution to nuclear shadowing in DIS. Figure from Ref. [28].

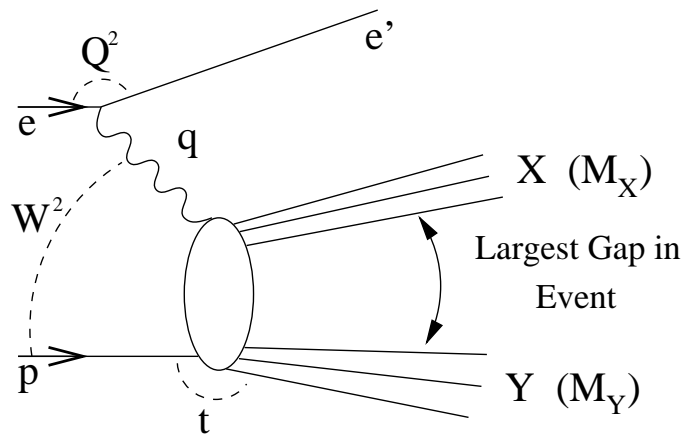


Figure 10: The diagram of a process with a rapidity gap between the systems X and Y. The projectile nucleus is denoted here as p. Figure from Ref. [3].